Available online at www.sciencedirect.com
ScienceDirect
Progress in Natural Science 18 (2008) 953–963
Progress in Natural Science
www.elsevier.com/locate/pnsc

A novel method of systematic error compensation for a position and orientation system

Xiuxiao Yuan *

School of Remote Sensing and Information Engineering, Wuhan University, Wuhan 430079, China

Received 28 November 2007; received in revised form 22 January 2008; accepted 4 February 2008

Abstract

A novel method is introduced for self-calibration and elimination of systematic errors for a position and orientation system (POS). The method uses a combined bundle block adjustment with POS data (named the POS-supported bundle block adjustment) without a calibration field. On the basis of delivering strict observation equations for POS data, the specific scheme of compensating the translation and drift systematic errors in a POS is given, and a prototype system WuCAPS is developed. The effects of eliminating POS systematic errors using the POS-supported bundle block adjustment for different ground control conditions are tested using two sets of actual aerial photos. The first set was taken over a flat region in the suburbs of the city of Yingkou in China and tested at a scale of 1:2500. The second set was taken over a high mountainous region in the desert region of Xinjiang in China and tested at a scale of 1:32,000. The empirical results verified that the POS systematic errors can be completely eliminated and the photo elements of exterior orientation obtained by the POS-supported bundle block adjustment can satisfy the requirements of aerial photogrammetric topographic mapping when four full ground control points (GCPs) are emplaced in the corners of the adjustment block for large-scale images of flat regions, but only one full GCP emplaced in the center of the adjustment block is needed for medium-small scale images of mountainous regions. This not only demonstrates the validity of the established mathematical model and the feasibility of the method proposed in this paper, but also avoids the use of a special calibration field. Therefore, it can simplify the existing POS operation rules and dramatically save on practical application costs, laying the theoretical foundation for widespread use of POS.

Keywords: Position and orientation system (POS); Systematic error; POS-supported bundle block adjustment; Self-calibration; Accuracy

1. Introduction

In the late 1990s, an integrated global positioning/inertial navigation system (GPS/INS) was first used in aerial remote sensing in the United States of America, Germany and Canada to obtain the position and attitude of a sensor, that is, the image orientation parameters are determined at the time of exposure. The aim is for aerial photogrammetry to perform direct georeferencing (DG) with the obtained image orientation parameters making aerial triangulation unnecessary [1,2].

However, direct use of image orientation parameters determined by a position and orientation system (POS) in aerial photogrammetry requires not only far more complex and difficult aerial photography than in traditional photogrammetry, but also complicated off-line data processing. Fig. 1 represents the common work flow for image orientation parameters obtained with a POS.

The original reason for applying a POS to aerial photogrammetry is that the space intersection can directly make use of image orientation parameters to obtain 3D ground coordinates of object points, i.e. direct sensor orientation. It can be seen from Fig. 1 that the key procedure is making a rigorous POS systematic error calibration using the calibration field to eliminate the space offset and boresight

* Tel.: +86 02768778083; fax: +86 02768778086.
E-mail address: yxxqxhyw@public.wh.hb.cn

1002-0071/$ - see front matter © 2008 National Natural Science Foundation of China and Chinese Academy of Sciences. Published by Elsevier Limited and Science in China Press. All rights reserved.
doi:10.1016/j.pnsc.2008.02.005

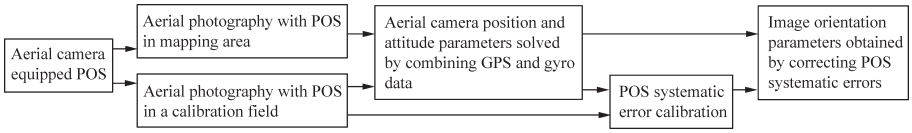

Fig. 1. Flowchart of image orientation parameters determined with a POS.

misalignment of the POS to improve the accuracy of image orientation parameters [3–5]. The disadvantages for the current calibration method are as follows. First, the calibration field and mapping projects are usually in different areas, so the terrain and environment conditions for aerial photography will be different. Second, the two areas usually cannot be photographed during the same flight mission due to air supervision and weather conditions. Third, it is difficult to take images over the calibration field in every real flight mission. Fourth, the POS systematic error calibration and correction are accomplished in different data processing stages, that is to say, the calibration must be made before the correction, hence they are separate processes. Theoretically speaking, the POS systematic error calibration for the calibration field cannot reflect all systematic errors for image orientation parameters obtained by a POS even through the most rigorous calibration and correction, and some residual errors still exist [6,7]. As a result, the digital orthophoto map can be made directly by image orientation parameters obtained by the POS [8,9], but there will be larger vertical parallax when stereo models are reconstructed using image orientation parameters and the height accuracy cannot satisfy the requirement of large scale topographic mapping [10]. Therefore, a bundle block adjustment should be made, combined image orientation parameters obtained by the POS and photogrammetric observations [11], so as to improve the accuracy of 3D ground coordinates of all object points and exterior orientation elements of images.

To thoroughly eliminate POS systematic errors and simplify the work flow of obtaining image orientation parameters with a POS, this paper puts forward a novel method of self-eliminating POS systematic errors in a POS-supported bundle block adjustment without the use of a special calibration field for error calibration. The main features of the method are that the POS data containing systematic errors are regarded as weighted observations for import into the bundle block adjustment, the translation and drift errors in positioning with a GPS and orientating with an inertial measurement unit (IMU) are well considered, a proper systematic error compensation model with additional parameters is proposed for the self-calibration adjustment and for eliminating POS systematic errors, and the 3D coordinates of all object points and the exterior orientation elements of images are gained to satisfy photogrammetric requirements. Therefore, based on the basic theory of bundle block adjustment, this paper establishes the error equations of the self-calibration POS-supported bundle block adjustment with additional parameters by analyzing the rigorous geometric relationship between image orientation parameters obtained by the POS and exterior orientation elements of images, and an adjustment prototype system named WuCAPS is developed. After aerial imagery, the validity of the mathematical model established and the effectiveness of eliminating the POS systematic errors are verified by comparing the results of the bundle block adjustment with calibrated and uncalibrated orientation parameters obtained by the POS, respectively. Furthermore, feasible operation advice is given for the method in the practical application, simplifying the POS operation rules and saving the use costs by analyzing the accuracy of the POS-supported bundle block adjustment for different ground control conditions.

2. Principle of POS systematic error compensation in bundle block adjustment

2.1. Rigorous geometric relationship of POS measurements

Fig. 2 represents the central perspective principle for the POS. Because the GPS antenna is mounted on top of the aircraft and the IMU is equipped on the camera, there is a lever arm effect for the antenna phase center A, IMU geometric center I and perspective center S. Furthermore, the IMU body coordinate system $I - x_I y_I z_I$ and camera coordinate system $S - uvw$ are not totally parallel due to limitations of installation and there is a tiny direction shift $\varphi_I,\omega_I,\kappa_I$ between the respective axes in the two coordinate systems, which is known as boresight misalignment [12].

Assuming that image point p has the coordinates (x, y) in the photographic coordinate system $o - xy$, and the cor-

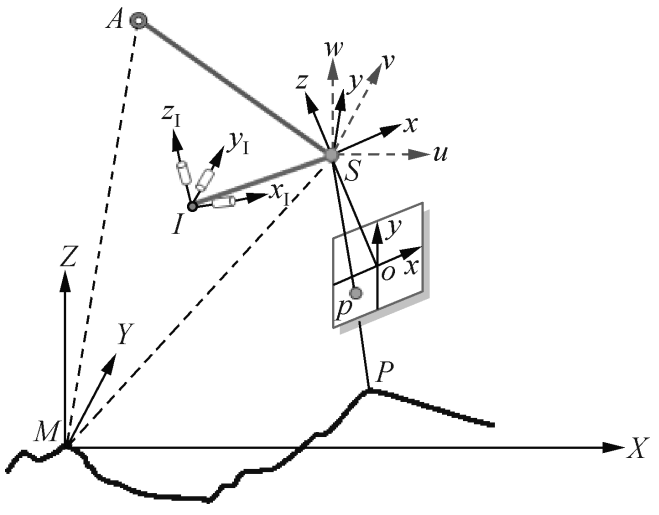

Fig. 2. Sketch map of the central projection principle for the POS.

responding object point P has the coordinates (X, Y, Z) in the ground coordinate system $M - XYZ$, then points p and P should in theory satisfy the collinearity equations [13]:

$$\begin{cases} x = -f\dfrac{a_1(X-X_s)+b_1(Y-Y_s)+c_1(Z-Z_s)}{a_3(X-X_s)+b_3(Y-Y_s)+c_3(Z-Z_s)} \\ y = -f\dfrac{a_2(X-X_s)+b_2(Y-Y_s)+c_2(Z-Z_s)}{a_3(X-X_s)+b_3(Y-Y_s)+c_3(Z-Z_s)} \end{cases} \tag{1}$$

where f represents the camera principal length, X_s, Y_s, Z_s represent ground coordinates of the perspective center S in the ground coordinate system $M - XYZ$, and a_1, a_2, $\ldots, c_3$ represent cosine values of image angle elements of the exterior orientation, that is

$$\mathbf{R} = \begin{bmatrix} a_1 & a_2 & a_3 \\ b_1 & b_2 & b_3 \\ c_1 & c_2 & c_3 \end{bmatrix} = \begin{bmatrix} \cos\varphi\cos\kappa - \sin\varphi\sin\omega\sin\kappa & -\cos\varphi\sin\kappa - \sin\varphi\sin\omega\cos\kappa & -\sin\varphi\cos\omega \\ \cos\omega\sin\kappa & \cos\omega\cos\kappa & -\sin\omega \\ \sin\varphi\cos\kappa + \cos\varphi\sin\omega\sin\kappa & -\sin\varphi\sin\kappa + \cos\varphi\sin\omega\cos\kappa & \cos\varphi\cos\omega \end{bmatrix} \tag{2}$$

In Fig. 2, the phase center of the GPS antenna is shown as A. Its coordinates are (X_A, Y_A, Z_A) in the ground coordinate system. If the antenna offset in the ideal camera coordinate system is (u, v, w), then the transformation is accomplished with orientation matrix $\mathbf{R}$ consisting of three image rotation angles ϕ,ω,κ. Thus, the following relationship can be concluded [14].

$$\begin{bmatrix} X_A \\ Y_A \\ Z_A \end{bmatrix} = \begin{bmatrix} X_S \\ Y_S \\ Z_S \end{bmatrix} + \mathbf{R}\cdot\begin{bmatrix} u \\ v \\ w \end{bmatrix} \tag{3}$$

From Fig. 2, it is seen that the coordinate system $I - x_I\, y_I\, z_I$ can be considered as the coordinate system $S - uvw$ after rotating $\varphi_I,\omega_I,\kappa_I$ around axes v,u,w, sequentially. When the attitude angles of the camera determined by the IMU are φ',ω',κ', the orthogonal transformation matrix $\mathbf{R}_{\mathrm{IMU}}$ can be represented as [15]

$$\mathbf{R}_{\mathrm{IMU}} = \mathbf{R}\cdot\mathbf{R}_B^{\mathrm{T}} \tag{4}$$

where $\mathbf{R}_{\mathrm{IMU}} = \mathbf{R}_{\varphi'}\mathbf{R}_{\omega'}\mathbf{R}_{\kappa'}, \mathbf{R}_B = \mathbf{R}_{\varphi_{\mathrm{I}}}\mathbf{R}_{\omega_{\mathrm{I}}}\mathbf{R}_{\kappa_{\mathrm{I}}}$.

Following Eq. (2), replacing φ,ω,κ with φ',ω',κ', and setting

$$\mathbf{R}\cdot\mathbf{R}_B^{\mathrm{T}} = \begin{bmatrix} a'_1 & a'_2 & a'_3 \\ b'_1 & b'_2 & b'_3 \\ c'_1 & c'_2 & c'_3 \end{bmatrix},$$

gives

$$\begin{cases} \varphi' = -\mathrm{arctg}\left(\dfrac{a'_3}{c'_3}\right) \\ \omega' = -\arcsin(b'_3) \\ \kappa' = \mathrm{arctg}\left(\dfrac{b'_1}{b'_2}\right) \end{cases} \tag{5}$$

Eqs. (1), (3) and (5) express a rigorous geometric relationship between coordinates of image points, image orientation parameters determined by the POS and exterior orientation elements in aerial images with POS data. They are the theoretical foundation of the combined bundle adjustment for POS data and photogrammetric observations.

2.2. Systematic error model of observations obtained with a POS

There are three types of original observations in the POS-supported bundle block adjustment: image point coordinates, exposure station coordinates determined by the GPS and camera attitude parameters obtained by the IMU. The observations of image point coordinates commonly contain systematic errors owing to the influence of lens distortion, negative deformation, photo digitization and image matching. Generally, for a digitalized image, the Bauer model [16] with three additional parameters can adequately compensate systematic errors in the image point coordinates:

$$\begin{cases} \Delta x = s_1 x(x^2+y^2-100) - s_3 x \\ \Delta y = s_1 y(x^2+y^2-100) + s_2 x + s_3 y \end{cases} \tag{6}$$

Ackermann [17] found that GPS dynamic positioning based on carrier phase measurements generates systematic errors that have a linear relationship with flight time t when the continuous flight period does not exceed 15 min:

$$\begin{cases} \Delta X_A = a_X + (t-t_0)b_X \\ \Delta Y_A = a_Y + (t-t_0)b_Y \\ \Delta Z_A = a_Z + (t-t_0)b_Z \end{cases} \tag{7}$$

The camera attitude parameters obtained by the IMU will have bigger drifts but still follow a linear relationship with flight time t. According to Eq. (7), they can be corrected by

$$\begin{cases} \Delta\varphi' = a_\varphi + (t-t_0)b_\varphi \\ \Delta\omega' = a_\omega + (t-t_0)b_\omega \\ \Delta\kappa' = a_\kappa + (t-t_0)b_\kappa \end{cases} \tag{8}$$

where, t_0 in Eqs. (7) and (8) is the reference moment. When the drift is regarded as a block invariant or a strip invariant, t_0 may be the exposure time of the first image in the block or strip.

If Eqs. (6)–(8) are respectively substituted into Eqs. (1)–(3), the observation equations of the POS are made more rigorous.

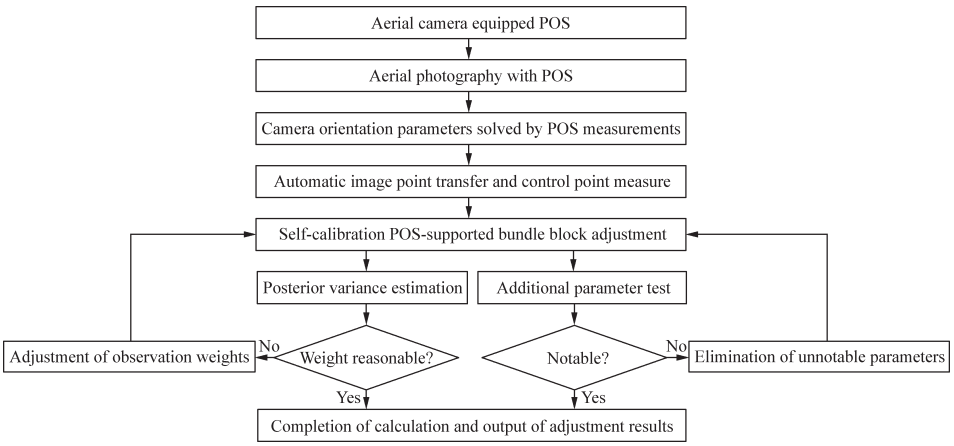

Fig. 3. Flowchart of self-calibration and elimination of POS systematic errors.

2.3. Scheme for compensating POS systematic errors

The image orientation parameters obtained by the POS and the image point coordinates can be combined in the adjustment according to the strict POS observation equations mentioned above. Here, the image point coordinates, exposure station coordinates determined by the GPS and camera attitude parameters obtained by the IMU are regarded as observations, and the 3D object coordinates and the six elements of exterior orientation for each image are regarded as unknowns. The error equations are then established after the linearization of Eqs. (1), (3) and (5). When the orientation parameters of m images taken over the adjustment block are determined by the POS and n image point coordinates are measured, there will be $2n + 6m$ error equations, thus the basic error equations of the POS-supported bundle block adjustment are formed. If their corresponding weights are consistent with their respective measuring accuracies of image point coordinates, the exposure station coordinates obtained by the GPS, and camera attitude parameters obtained by the IMU, then the most probable values of object space coordinates and the exterior orientation elements of the images can be solved using the least squares method. Because the cumulative errors of the POS measurements are considered in basic error equations and the proper compensation models of POS systematic errors are imported into Eqs. (6)–(8), the various rectification parameters of systematic errors are regarded as undetermined parameters in the block adjustment and as weighted observations in building virtual error equations to be included in the overall adjustment. The rectification parameters of systematic errors are solved simultaneously in the adjustment. When the adjustment has iterative convergence, the position translation errors and linear drift errors with time, generated by the POS, can be self-calibrated and self-eliminated, which achieve the purpose of improving the measuring accuracy of the exterior orientation elements of the images and accordingly avoid the special systematic error calibration of the POS using the calibration field. The specific solution procedure is shown in Fig. 3.

3. WuCAPS description

According to the above-mentioned basic error equations, the author adds two functional modules. The first is an automatic measurement of the digital images and the second is a POS-supported bundle block adjustment in the self-developed combined bundle block adjustment procedure WuCAPS (Wuhan Combined Adjustment Program System for photogrammetric and non-photogrammetric observations). Object-oriented Visual C^{++} and Visual Fortran programming languages in a Windows environment were used. Fig. 4 shows the main menu of the Windows version of WuCAPS.

WuCAPS is a software package suitable for the combined adjustment of photogrammetric and non-photogrammetric observations developed by the author. It starts from collinearity equations, combines the stochastic model based on statistical theory with the strict mathematical model of the combined bundle block adjustment, and then uses a series of special algorithms developed in WuCAPS. The strictness of theory and flexibility of practical application mean that WuCAPS will be widely used both in scientific research and in practical production. At present, WuCAPS is used as a means of control point determination for aerial photogrammetry in China. The main functions are listed as follows.

(1) Point transfer by automatic image matching and measurement by manual stereoscopic observation.
(2) Stereo models reconstructed using given elements of exterior orientation to implement direct sensor orientation.
(3) Block adjustment by trips.
(4) Self-calibration bundle block adjustment with additional parameters including bundle block adjustment with ground control points (GCPs) regarded as real

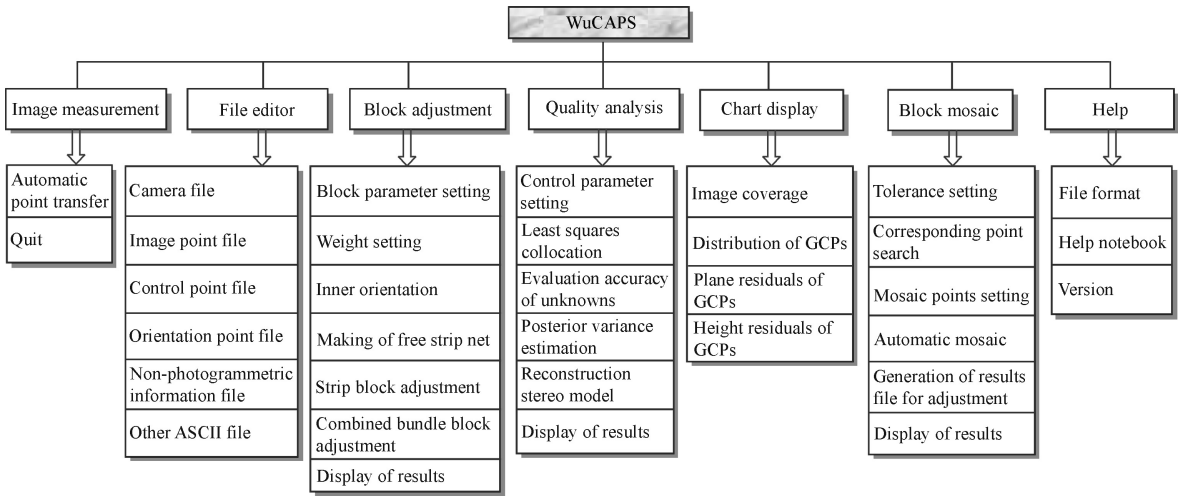

Fig. 4. Main menu of WuCAPS.

values, self-calibration bundle block adjustment with GCPs regarded as real values, bundle block adjustment with GCPs regarded as weighted observations, self-calibration bundle block adjustment with GCPs regarded as weighted observations.

(5) Combined bundle adjustment with GPS/IMU navigation data and/or geodetic observations including combined adjustment with geodetic observations such as leveling, spatial distances, horizontal angles and vertical angles, GPS-supported bundle block adjustment with 3D GPS-determined positions of camera centers, POS-supported bundle block adjustment with POS-determined orientations of camera.

(6) Automatic detection and rejection of blunders including automatic detection of blunders in the fiducial mark observations by data-snooping approach during inner orientation, and efficient elimination of blunders in image observations, exposure station coordinates obtained by the GPS and tie point coordinates between strips by the varying weight iteration method.

(7) Compensation of systematic errors including compensation of systematic errors for tie points in images using Bauer model/Ebner model/Brown model [16] with additional parameters, compensation of the systematic errors for image orientation parameters obtained by the POS using a model with translation and drift additional parameters, registering of adjusted coordinates of photogrammetric points with the coordinate system defined by the GCPs using least squares collocation after conventional bundle adjustment according to the coordinate residuals between GCPs from the photogrammetric adjustment and field survey.

(8) Evaluation of the theoretical accuracy of unknowns and calculation of the reliability of observations.

(9) Automatic adjustment of measurement weights by estimating the posterior variance components.

(10) Drawing of the chart of image coverage and a residual sketch of GCPs in the adjustment block.

(11) Semi-automatic mosaic of densification subprojects.

4. Experiments

4.1. Empirical test design

This study used WuCAPS as a test platform in experiments on flat terrain in Yingkou City, Liaoning Province, and a desert region with high mountainous terrain in Xinjiang, China. The main technical parameters of the empirical images are given in Table 1. The distribution of the images and GCPs in the empirical blocks is shown in Fig. 5.

The two empirical blocks are only a small part of the two-region mapping project. Flat and high mountain areas were selected here based on previous experiences in photogrammetric point determination. Generally speaking, the requirement is rigorous coordinate accuracy of photogrammetric points, especially the height accuracy for flat terrain. It is usually difficult to meet accuracy requirements in the photogrammetric block adjustment for flat terrain, whereas it is easier to satisfy the requirements for high mountainous regions. Each mapping region has its respective special calibration field. Each calibration field comprises two strips with 12 images in each strip. The calibration fields are not in the selected empirical blocks.

After all negatives were scanned with a resolution of 21 μm to digital images, the WuCAPS system was used for automatic point transfer. The corresponding image coordinates of all GCPs were measured manually in the stereoscopic mode. The root mean square error (RMSE) of all image coordinates was statistically better than ±6.0 μm according to the results of the consecutive relative orientation with conditions for model connection and the function of gross errors eliminated by WuCAPS.

Table 1
Technical parameters of images in empirical blocks

	Test 1	Test 2
Date	November 2004	September 2005
Aircraft	Yun-12 made in China	Yun-12 made in China
Aerial camera	Leica RC-30	Leica RC-30
Flight control system	Track Air	CCNS 4
POS system	POS AV 510	POS AV 510
GPS receivers	Ashtech	Trimble 5700
Film	Kodak 2444	Kodak 2402
Principal length	153.84 mm	154.06 mm
Frame	23 cm × 23 cm	23 cm × 23 cm
Photo scale	1:2,500	1:32,000
Longitudinal overlap	61%	64%
Lateral overlap	32%	33%
Strips	9	9
Number of photographs	189	180
GCPs	71	34
Object points	2826	2440
Area	4 × 5 km	47 × 52 km
Maximum terrain undulation	38.0 m (flat)	723.4 m (high mountainous)
GPS refresh rate	2 s	1 s
GPS initialization	10 min	5 min
GPS static observation	5 min	5 min
Antenna-camera offset	0.303 m, −0.110 m, −2.029 m	−2.015 m, −0.030 m, 3.102 m
IMU-camera offset	0.000 m, 0.200 m, −0.559 m	0.000 m, −0.201 m, 0.407 m

The GCPs were determined by combined static GPS net surveying, and the planimetric coordinates were transformed to the Xian geodetic coordinate system 1980 under Gauss–Kruger projection, while the elevation coordinate system took national height datum. The GCPs were measured by two surveying and mapping companies, and the planimetry accuracy was better than ±0.1 mm on the map in two empirical blocks. In Test 1, elevation was measured by a leveling survey, and the accuracy was higher than ±0.1 m. In Test 2, elevation was measured by a GPS geoid fitting method with an accuracy better than ±0.5 m.

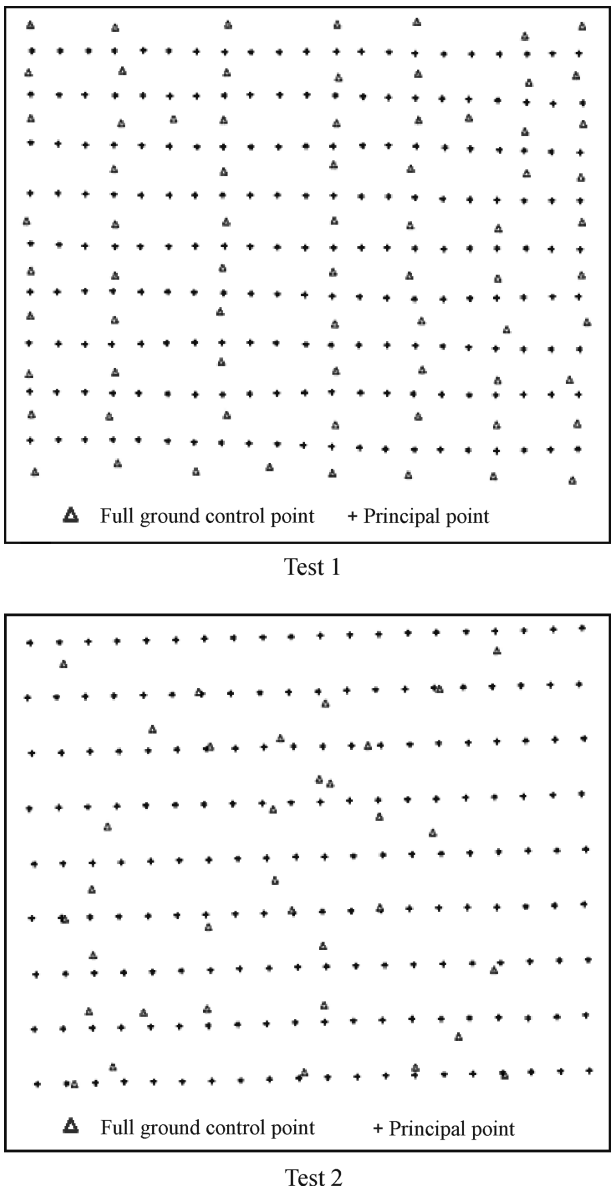

Fig. 5. Distribution of images and GCPs in empirical blocks.

4.2. Results of the bundle block adjustment

Firstly, the measurements acquired by GPS/IMU for the two empirical blocks were processed, respectively, using POS data postprocess software POSPac [18], to determine the positions and attitudes of aerial cameras (referred to as uncalibrated). According to POS operation rules, the POS systematic errors in the two mapping projects were then calibrated individually using their corresponding calibration fields. The six elements of exterior orientation for each image could be determined after systematic error correction and coordinate transformation (referred to as calibrated).

The two types of orientation parameters (that is, calibrated and uncalibrated) were each used to support the bundle block adjustment. Owing to the use of various types of observations, such as image point coordinates, GCP coordinates, the exposure station coordinates determined by GPS and the attitudes obtained by IMU, each type of measurement was regarded as independent observations and had a respective weight based on its surveying accuracy. The weights were then adjusted based on the posterior variance estimation in the block adjustment. Furthermore, to obtain the best adjustment results, four kinds of ground control plans were adopted, which emplaced four full GCPs in the four corners around the empirical block, two full GCPs in the two diagonals around the empirical block, one full GCP in the central region or no GCPs. The accuracies of the POS-supported bundle block adjustment under the different ground control conditions were compared. In the end, the theoretical accuracy and practical accuracy of block adjustment were evaluated, respectively, using the propagation law of errors

and a large number of ground check points. The results are shown in Table 2. Taking Test 1 as an example, Fig. 6 draws the residual sketch of GCPs under both circumstances with GCPs in the four corners around the empirical block and without any GCP.

In Table 2, the theoretical accuracy is calculated by posterior mean square error of the unit weight σ_0 and the inverse matrix $\mathbf{Q}_{XX}$ (that is, the weight reciprocal matrix) of the normal equation's coefficient matrix of the block adjustment [19]. The theoretical accuracy formula of unknown individual is

$$m_i = \sigma_0\sqrt{Q^i_{XX}}, \quad (i = X, Y, Z) \tag{9}$$

For the photogrammetric block adjustment containing n object points, we can use

$$\begin{aligned} \bar{m}_{XY} &= \sigma_0\sqrt{\frac{1}{n}\sum_{i=1}^{n}(Q^i_{XX} + Q^i_{YY})} \\ \bar{m}_Z &= \sigma_0\sqrt{\frac{1}{n}\sum_{i=1}^{n}Q^i_{ZZ}} \end{aligned} \tag{10}$$

to express the overall theoretical accuracy for planimetry and the determination of elevation. However, the practical accuracy is the average mean square error of n check points calculated by the difference between the adjusted coordinates and field surveying coordinates.

$$\begin{aligned} \bar{\mu}_{XY} &= \sqrt{\frac{1}{n}\sum_{i=1}^{n}(\Delta X_i^2 + \Delta Y_i^2)} \\ \bar{\mu}_Z &= \sqrt{\frac{1}{n}\sum_{i=1}^{n}\Delta Z_i^2} \end{aligned} \tag{11}$$

From Table 2 and Fig. 6, the following conclusions can be drawn:

(1) In the block with GCPs, the results using the image orientation parameters to support the bundle block adjustment have no essential differences, whether the calibration and rectification of the POS systematic errors uses a calibration field. The larger the image scale is, the more GCPs there are, the lower the resolution of the hypsography is, and the smaller the difference will be. For the high mountainous region at a medium scale of 1:32,000, the difference in the planimetry RMSE is only ±0.085 m and that for the height RMSE is ±0.165 m, from using the two adjustment methods. This difference can be entirely ignored as for topographic mapping at medium-small scale.

(2) The accuracy of the POS-supported bundle block adjustment without any GCP depends entirely on the accuracy of the orientation parameters obtained by POS. The calibrated and uncalibrated orientation parameters obtained by the POS have been, respectively, used in the bundle block adjustment. The difference in the planimetry RMSE between the two is less than ±0.150 m but that for the height RMSE is ±4.444 m. The reason is the accuracy of the exposure station coordinates determined by the GPS is better for planimetry but poorer for elevation, and the attitude parameters of the aerial camera determined by IMU has greater boresight misalignment. Hence, the results will inevitably contain larger systematic errors using measurements obtained directly from the POS to implement the bundle block adjustment, as in the example shown in Fig. 6(a) and (b). In additional, the difference is artificial distinction between Test 1 and Test 2. The reason is that two sets of images were taken from two different projects and their orientation parameters were obtained by two POSs. The boresight misalignments of both systems

Table 2
Accuracy of the POS-supported bundle block adjustment

Image	GCPs	Elements of exterior orientation obtained by POS	σ_0 (μm)	Check points	Maximal residuals of check points (m)				Practical precision (m)				Theoretical precision (m)			
					X	Y	XY	Height	X	Y	XY	Height	X	Y	XY	Height
Test 1	4	Calibrated	6.0	67	−0.202	−0.287	0.224	0.256	0.097	0.094	0.121	0.099	0.017	0.023	0.029	0.091
		Uncalibrated	6.1	67	−0.204	−0.311	0.247	−0.237	0.095	0.089	0.120	0.091	0.018	0.023	0.029	0.093
	2	Calibrated	5.5	69	−0.202	0.320	0.334	−0.375	0.078	0.156	0.174	0.194	0.034	0.040	0.052	0.123
		Uncalibrated	5.5	69	−0.204	0.330	0.335	−0.375	0.078	0.159	0.177	0.196	0.034	0.040	0.052	0.123
	1	Calibrated	5.4	70	0.328	−0.344	0.401	0.504	0.105	0.154	0.186	0.186	0.063	0.075	0.098	0.166
		Uncalibrated	5.4	70	0.328	−0.353	0.409	0.447	0.105	0.156	0.188	0.164	0.063	0.075	0.098	0.166
	0	Calibrated	5.8	71	−0.616	0.799	0.923	1.466	0.396	0.609	0.726	0.634	0.202	0.199	0.284	0.206
		Uncalibrated	5.9	71	0.783	−0.436	0.896	−5.831	0.573	0.194	0.605	5.078	0.205	0.201	0.287	0.209
Test 2	4	Calibrated	6.1	30	−1.399	1.554	1.969	−1.569	0.723	0.709	1.012	0.724	0.180	0.231	0.341	0.336
		Uncalibrated	6.1	30	−1.443	−1.394	1.544	−1.665	0.665	0.661	0.937	0.793	0.231	0.341	0.412	0.336
	2	Calibrated	6.1	32	1.607	1.891	2.482	−1.937	0.826	0.983	1.284	0.809	0.259	0.386	0.465	0.362
		Uncalibrated	6.1	32	1.311	1.816	1.932	−2.153	0.773	0.950	1.225	0.974	0.259	0.386	0.465	0.362
	1	Calibrated	6.1	33	−2.522	−1.991	2.766	1.918	1.166	0.645	1.332	0.910	0.249	0.373	0.448	0.380
		Uncalibrated	6.1	33	−2.455	−2.025	2.688	1.924	1.064	0.650	1.247	1.018	0.250	0.373	0.448	0.380
	0	Calibrated	6.1	34	−1.771	−2.019	2.116	3.546	0.720	0.647	0.968	2.293	0.676	0.713	0.983	0.711
		Uncalibrated	6.1	34	−1.653	−1.769	1.849	4.723	0.619	0.586	0.852	3.559	0.675	0.716	0.984	0.711

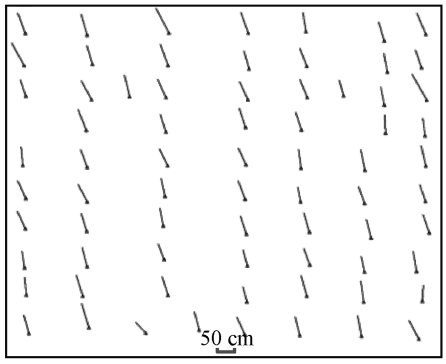

(a) Planimetry residuals of GCPs using uncalibrated orientation parameters obtained by the POS to support bundle block adjustment (without GCPs)

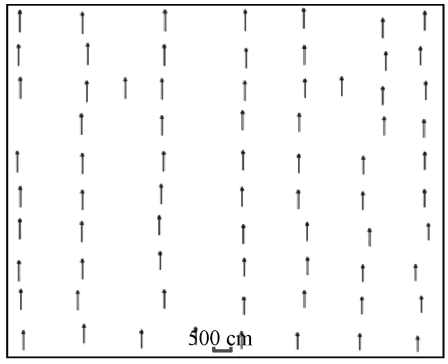

(b) Height residuals of GCPs using uncalibrated orientation parameters obtained by the POS to support bundle block adjustment (without GCPs)

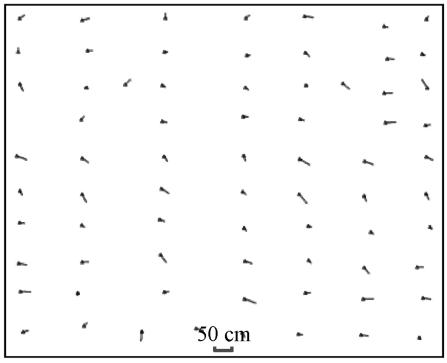

(c) Planimetry residuals of GCPs using calibrated orientation parameters obtained by the POS to support bundle block adjustment (without GCPs)

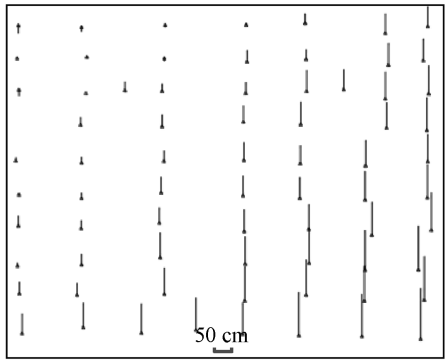

(d) Height residuals of GCPs using calibrated orientation parameters obtained by the POS to support bundle block adjustment (without GCPs)

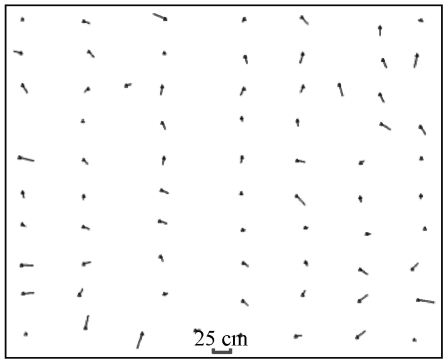

(e) Planimetry residuals of GCPs using uncalibrated orientation parameters obtained by the POS to support bundle block adjustment (with 4 full GCPs in the four corners of the area)

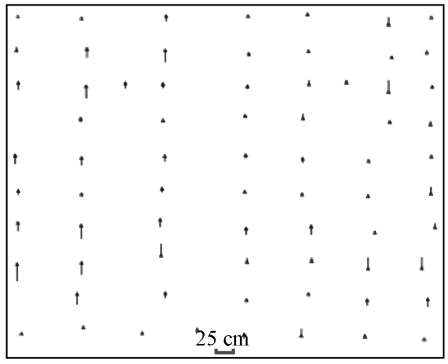

(f) Height residuals of GCPs using uncalibrated orientation parameters obtained by the POS to support bundle block adjustment (with 4 full GCPs in the four corners of the area)

Fig. 6. Distribution of coordinate residuals for check points in Test 1.

are obviously distinct. The systematic errors of two sets of image orientation parameters are not same and are very difficult to compensate during POS-supported bundle block adjustment without any GCP. Therefore, the accuracies of photogrammetric points are very different in two test projects. However, by calibrating POS data using the calibration field, the primary systematic errors can be eliminated and the accuracy of orientation parameters improved. The planimetry coordinates of photogrammetric points will no longer contain systematic errors if the orientation parameters obtained by the POS are used to support the bundle block adjustment after calibration, as shown in Fig. 6(c). The height accuracy of photogrammetric points is also significantly improved, but as can be seen from Fig. 6(d), there are still systematic residuals present. This is because the drift parameters calibrated by the calibration field can only reflect the overall errors in the POS, but not the systematic errors in the orientation parameters.

The effect of the residual error on the block adjustment is still very large. However, when the uncalibrated orientation parameters obtained by the POS are used directly to implement the bundle block adjustment, and if the translation and drift compensation models are used for the error equations to implement the self-calibration adjustment, the systematic errors can be totally eliminated. Comparing Fig. 6(e) with Fig. 6(c), and Fig. 6(f) with Fig. 6(d), the effect is very obvious. This shows that the systematic errors for orientation parameters obtained by the POS cannot be totally eliminated when calibration uses a calibration field, and it is better to use a self-calibration POS-supported bundle block adjustment and eliminate the systematic errors of orientation parameters determined by the POS.

(3) As far as theoretical accuracy is concerned, the results are exactly the same and are of a very high level when using the orientation parameters to support bundle block adjustment, no matter they are calibrated or not. This shows a high accuracy potential of the POS-supported bundle block adjustment. However, the practical accuracy is obviously worse than the theoretical accuracy for the POS-supported bundle block adjustment. The reason is that the theoretical accuracy only reflects the structure of the block and the error in the mathematical model, which is a measurement of the limit that the accuracy can attain in the use of the aerial photogrammetric block adjustment. However, the practical accuracy not only embodies the error of the mathematical model, but also synthetically embodies the combined effects of residual errors such as the unallocated interpretation errors of GCPs, the matching error for homologous points and the measurement errors obtained with the POS. In the experiment, all the image coordinates were acquired by automatic image matching technology and the measurement accuracy could achieve a sub-pixel level. All GCPs were outstanding object points and were measured manually in the stereoscopic mode, so the identification of image points would inevitably contain a small translation error. Furthermore, there is film distortion, image scanning errors, and other considerations. Although there are systematic errors in image point coordinates, the drift compensation models for the positioning by the GPS and orientating by the IMU are considered in the block adjustment. The results of the adjustment still contain residual errors that lead to the practical accuracy being not entirely consistent with the theoretical accuracy, and the difference between them is quite large for the horizontal position. Furthermore, owing to the image point coordinates of GCPs being measured manually in the stereoscopic mode, there can also be differences tangent to the ground surface. Especially for Test 1 with the flat terrain, a small deviation in position is not sufficient to cause a large height error, so the practical accuracy is very close to the theoretical accuracy for the elevation of object points. However, for Test 2 with the high mountainous region, the check points are distributed on different objects and the image scale is smaller, so the image interpretation will be difficult. This leads to the practical accuracy being obviously lower than the theoretical accuracy for the elevation of photogrammetric points.

4.3. Feasibility analysis of topographic mapping application

According to the existing Specifications for Aerophotogrammetric Office Operation, the two above-mentioned empirical blocks belong to flat and high mountainous regions, respectively. The images for Test 1 and Test 2 can be used for topographic mapping at a scale of 1:500–1:2,000 and 1:10,000, respectively. The topographic control points in Test 1 must be determined using a full field survey method instead of aerial triangulation. The following conclusions can be deduced by analyzing the results in Table 2.

(1) The accuracy of the POS-supported bundle block adjustment improves with an increase in the number of GCPs. When the number of GCPs increases from 1 to 4, the improvement in accuracy is not large. When emplacing 4 full GCPs in the four corners of the adjusted block, the accuracy of pass points can satisfy the requirements of topographic mapping.

(2) For Test 1, the accuracy of the POS-supported bundle block adjustment with 4 full GCPs in the four corners of the adjusted block is better than ± 0.121 m for planimetry and better than ± 0.100 m for elevation determination. The maximum coordinate residuals of 68 check points are 0.247 m for planimetry and -0.256 m for elevation, which satisfy the existing specifications' tolerance of check point coordinate inconsistencies being less than 0.25 m for planimetry and less than 0.30 m for elevation determination for flat topographic mapping at a 1:500 scale [20]. Other ground control plans cannot guarantee the accuracy of pass point coordinates will satisfy the requirements of topographic mapping.

(3) For Test 2, the accuracy of the POS-supported bundle block adjustment with 4 full GCPs in the four corners of the adjusted block almost reaches ± 1.0 m for planimetry and is better than ± 0.8 m for elevation determination. The maximum coordinate residuals of 25 check points are 1.969 m for planimetry and -1.665 m for elevation determination, which satisfy the specifications' tolerance of check point coordinate inconsistencies being less than 4.0 m for planimetry and less than 2.2 m for elevation determination for high mountain region topographic mapping at a 1:10,000 scale [21]. However, even emplacing only

one full GCP in the central region of the adjusted block, the accuracy of check points can still satisfy the requirements of topographic mapping.

In summary, as far as topographic mapping is concerned, the uncalibrated orientation parameters determined by the POS can be used to support the bundle block adjustment if aerial triangulation is first used, rather than reconstructing the stereo model later, and emplacing four full GCPs in the four corners of the adjusted block, irrespective of the size of the block. This can not only save the use of many GCPs, but also overcome the problem of greater vertical parallax generated when a stereo model is reconstructed using orientation parameters determined by the POS at present. Hence, the method can play an important role in topographic mapping especially in regions that are difficult to access.

5. Conclusions

A novel method was proposed for self-calibrating and eliminating systematic errors of image orientation parameters determined by a POS. The following conclusions were verified by experiments on actual aerial images at 1:2,500 and 1:32,000 scales using the self-developed POS-supported bundle block adjustment system WuCAPS.

(1) The basic error equations of the POS-supported bundle block adjustment with additional parameters established in this paper are found to be sound.
(2) When the image orientation parameters obtained by the POS are used for stereoscopic observation, the emplacement of a special calibration field is not needed to calibrate POS systematic errors. The systematic errors can be compensated and eliminated in the POS-supported bundle block adjustment by adding proper additional parameters. This will not increase the operational difficulty and workload of existing aerial photogrammetry, but can solve the problem of the greater vertical parallax for models generated with a POS at present, which cannot satisfy the accuracy requirements of topographic mapping at a large scale. When the method proposed in this paper is used, the POS-supported aerial photography can follow conventional aerial photography specifications but without the need for a calibration field.
(3) To guarantee the POS systematic errors which can be completely eliminated in the POS-supported bundle block adjustment, it is necessary in the large scale topographic mapping of flat regions to emplace four full GCPs in the four corners of the adjustment block. The size of the block can be set based on the specification and the number of GCPs does not change whether the block size is big or small. This can enormously reduce the workload in an aerial photogrammetric field control survey. For medium-small scale topographic mapping in a high mountainous region, at least one full GCP needs to be emplaced in the central region for the adjustment to ensure the vertical accuracy of pass points. With the national high-grade GPS network completely emplaced and operational, as long as the photogrammetric adjustment blocks are reasonably plotted, then aerial triangulation can be carried out without a field control survey.

Acknowledgements

This work was supported by the National Natural Science Foundation of China (Grant Nos. 40771176 and 40721001) and the Program for New Century Excellent Talents in University (Grant No. NCET-04-0662). The empirical data acquisition is supported by the Institute of Remote Sensing Applications in Chinese Academy of Sciences, Zhongfei General Aviation Company, Liaoning Jingwei Surveying and Mapping Technology INC, Siwei Aviation Remote Sensing Co. Ltd., and others. This support is gratefully acknowledged. Dr. Shunping Ji, Jianhong Fu and Yang Ming participated in the experiments. Prof. Zhilin Li of the Hong Kong Polytechnic University gave many constructive suggestions in the writing and Zhenli Wu helped improve the English. The author would like to express his hearty gratitude for their efforts.

References

[1] Cramer M, Stallmann D, Haala N. Direct georeferencing using GPS/inertial exterior orientations for photogrammetric applications. Int Arch Photogramm Remote Sens 2000;33(B3):198–205.
[2] Li XY. Principle, method and practice of IMU/DGPS-based photogrammetry. Ph.D. Thesis, Information Engineering University, Zhengzhou, China; 2005.
[3] Bäumker M, Heimes FJ. New calibration and computing method for direct georeferencing of image and scanner data using the position and angular data of a hybrid inertial navigation system. In: Proceedings of OEEPE workshop on integrated sensor orientation, Hanover, Germany; 2002.
[4] Cramer M, Stallman D. System calibration for direct georeferencing. Int Arch Photogramm Remote Sens 2002;34:79–84.
[5] Jacobsen K. Calibration aspects in direct georeferencing of frame imagery. In: Proceedings of Pecora 15/L and satellite information, ISPRS Commission I/IV, Spain; 2002.
[6] Madani M, Mostafa MMR. ISAT direct exterior orientation QA/QC strategy using POS data. In: Proceedings of OEEPE workshop on integrated sensor orientation, Hanover, Germany; 2001.
[7] Ressl C. The OEEPE test 'integrated sensor orientation' and its handling within the hybrid block-adjustment program ORIENT. In: Proceedings of OEEPE workshop on integrated sensor orientation, Hanover, Germany; 2001.
[8] Grün A, Baer S. Aerial mobile mapping-georeferencing without GPS/INS. In: Proceedings of the 3rd International symposium on mobile mapping technology, Cairo, Egypt; 2001.
[9] Heipke C, Jacobsen K, Wegmann H. The OEEPE test on integrated sensor orientation-results of phase I. In: Proceedings of photogrammetric week, Stuttgart, Germany; 2001. p. 195–204.
[10] Yuan XX. Some investigations of image orientation in aerial photogrammetry. Adv Earth Sci 2007;22(8):828–34, [in Chinese].

[11] Greening T, Schickler W, Thorpe A. The proper use of directly observed orientation data: aerial triangulation is not obsolete. In: Proceedings of 2000 ASPRS annual conference, Washington, DC, USA; 2000.
[12] Mostafa MMR. Digital multi-sensor system – calibration and performance analysis. In: Proceedings of OEEPE workshop on integrated sensor orientation, Hanover, Germany, 2001.
[13] Wang ZZ. Principle of photogrammetry (with remote sensing). Beijing: Publishing House of Surveying and Mapping; 1990.
[14] Yuan XX. Principle, software and experiment of GPS-supported aerotriangulation. Geo-Spatial Inform Sci 2000;3(1):24–33.
[15] Yuan XX, Yang F, Zhao Q, et al. Boresight calibration of airborne position and orientation system. Geomat Inform Sci Wuhan Univ 2006;31(12):1039–43, [in Chinese].
[16] Li DR, Yuan XX. Error processing and reliability theory. Wuhan: Press of Wuhan University; 2003, [in Chinese].
[17] Ackermann F. Practical experience with GPS-supported aerial triangulation. Photogramm Rec 1994;16(84):861–74.
[18] Applanix Product Outline. POSPac^{TM}Air. http://www.applanix.com/products/pospac_airborne_index.php, 2007.
[19] Li DR, Shan J. Quality analysis of bundle block adjustment with navigation data. Photogramm Eng Remote Sens 1989;55(12):1743–6.
[20] GB 7930-87. 1:500, 1:1000, 1:2000 Topographical maps specifications for aerophotogrammetric office operation. Beijing: Standards Press of China; 1998, [in Chinese].
[21] GB/T 13990-92. 1:5000, 1:10000 Topographical maps specifications for aerophotogrammetric office operation. Beijing: Standards Press of China; 1993, [in Chinese].